

## CROSS SECTIONS FOR PRODUCTION OF H(2*p*, 2*s*, 1*s*) BY ELECTRON COLLISIONAL DISSOCIATION OF H<sub>2</sub>

J. M. AJELLO

M-S 183-601, Jet Propulsion Laboratory, 4800 Oak Grove Drive, California Institute of Technology, Pasadena, CA 91109

D. E. SHEMANSKY

Lunar and Planetary Laboratory, University of Arizona, Tucson, AZ 85721

AND

G. K. JAMES

M-S 183-601, Jet Propulsion Laboratory, 4800 Oak Grove Drive, California Institute of Technology, Pasadena, CA 91109

Received 1990 May 29; accepted 1990 September 18

### ABSTRACT

We have measured the excitation function of H Ly $\alpha$  produced by dissociative excitation of H<sub>2</sub> at energies 10–700 eV. The branches of the reaction have been separated using analytic models to fit the measured total excitation function. Strong threshold resonances by triplet states account for the sharp cross section rise at threshold, 14.7 eV. Above thresholds to 25 eV the  $e^3\Sigma_u^+$  state makes the largest contribution to the H Ly $\alpha$  emission cross section by direct dissociation and predissociation of the  $d^3\Pi_u$  state. The excitation function displays structure at  $\sim 30$  eV which can be attributed to the production of fast ( $\approx 4$  eV) H(2*l*) atoms from doubly excited states. Above 50 eV predissociation of the singlet states (*D*, *D'*, *B''*) by the *B'* state accounts for the largest contribution of the H Ly $\alpha$  emission cross section. The yield of H(2*p*), H(2*s*), and H(1*s*) atoms contributing to the dissociation of H<sub>2</sub> into H(2*l*) and H(1*s*) atoms including cascade components was calculated from the measurements to be  $33\% \pm 5\%$ ,  $23\% \pm 4\%$ , and  $44\% \pm 6\%$ , respectively, at 100 eV.

*Subject headings:* atomic processes — molecular processes — transition rates

### 1. INTRODUCTION

Electron impact excitation of H<sub>2</sub> is an important part of physical chemistry in stellar atmospheres, molecular clouds, and planetary atmospheres. The absolute cross section of H Ly $\alpha$  by dissociative excitation of H<sub>2</sub> is also a secondary calibration standard for normalization of optical excitation function and spectral measurements in the laboratory. Dissociative excitation of H(2*l*) atoms occurs through several branches in electronically excited H<sub>2</sub> structure. The components of the total cross section have never been clearly separated. A quantitative separation of the basic branches in the total cross section is of interest to astrophysics because of distinct differences in exothermicity which affect thermodynamic considerations, particularly in molecular cloud and planetary atmospheric physics.

The absolute cross section for H Ly $\alpha$  emission from dissociative excitation has been used extensively in the past as a calibration standard. Several recent independent measurements of the cross section at 100 and 200 eV have produced a substantial downward revision from the value generally accepted prior to 1985 (see Shemansky, Ajello, & Hall 1985a). Ajello *et al.* (1988) have recommended the adoption of a value of  $7.3 \times 10^{-18}$  cm<sup>2</sup> at 100 eV, the mean of four recent determinations. The value  $11.8 \times 10^{-18}$  was in general use prior to 1985. The production of H(2*l*) and H(1*s*) atoms at 100 eV has been calculated in our analysis. A comparison of H(2*l*) production by Ajello *et al.* (1988) together with the study of H(2*p*) production from this work provides the H(2*p*), H(2*s*), and H(1*s*) yield. The source partitioning of the total cross section for production of H(2*p*) atoms has also been separated through knowledge of the shapes of the excitation functions established for relevant emission transitions in H<sub>2</sub>. We provide estimates of triplet, doubly excited, and singly excited state contributions

to the total. Triplet states dominate the H Ly $\alpha$  cross section near threshold. The near-threshold cross sections of many electronic states of H<sub>2</sub> are modified by resonance processes and can affect rates at low electron temperature. Quantitative measurements of the near threshold H<sub>2</sub><sup>-</sup> states affecting the H<sub>2</sub> singlet Rydberg series will be reported in the following paper.

The only previous work on the excitation of H Ly $\alpha$  in the threshold energy region is the electron-photon coincidence experiment by Böse & Linder (1979) who performed a measurement from 11 to 16 eV. Böse & Linder (1979) used an optical filter photometer arrangement with a bandpass from 112 to 130 nm. Their measurement included radiation from the Rydberg states with a threshold near 11 eV as well as H Ly $\alpha$  radiation. Previous work with vacuum UV (VUV) spectrometers by Mumma & Zipf (1971) and Vroom & de Heer (1969) have not concentrated on the threshold region.

In our experiment the low- and intermediate-energy region from 11 to 400 eV was studied at resolution high enough to avoid blending with nearby H<sub>2</sub> Werner and Lyman transitions. A modified Born approximation (Shemansky *et al.* 1985a, b) has been used to fit and extend the cross section measurements to arbitrary high energy for use in electron energy loss codes.

### 2. EXPERIMENTAL

The experimental apparatus and VUV calibration techniques have been described in detail in earlier publications (Ajello, Srivastava, & Yung 1982; Ajello *et al.* 1984; Ajello & Shemansky 1985; Ajello *et al.* 1989). Two independent systems have been used in the measurements. Each of these systems consists of an electron impact collision chamber in tandem with either one or two UV spectrometers, an extreme ultraviolet (EUV) spectrometer operating in the range 40–140 nm, and a far-ultraviolet (FUV) spectrometer effective over the 110–210

nm range. One system is a high-resolution apparatus with a spectral resolution capability of 0.02 nm. The other system is a low-resolution apparatus with a spectral resolution capability of 0.4 nm.

A magnetically collimated beam of electrons impacts a static gas sample at a pressure that can be varied from  $1 \times 10^{-7}$  to  $3 \times 10^{-4}$  torr. The cross section measurements were obtained at  $6 \times 10^{-6}$  torr pressure and with 100  $\mu$ A Faraday cup current in the collision chamber. The energy resolution is 0.3 eV. The instrument is automated for repetitive scans and interfaced with a computer. The electron gun is mounted on a rotatable table to allow a measurement of the angular distribution of the radiation field in order to correct the measured cross section for polarization effects. However, the measurements reported here were made at a  $90^\circ$  angle between electron beam axis and optic axis, since polarization is expected to be small for molecular dissociative excitation where many intermediate states contribute (Van Brunt & Zare 1968). At the appearance potential (AP) of 14.7 eV and near 50 eV, the polarization can be as large as 12% (Malcolm, Dassen, & McConkey 1979). The correction to the cross section is less than 4%. Vroom & de Heer (1969) have shown that in the case of H Ly $\alpha$  emission magnetic collimation by a field of 50 G does not produce significant  $2s$ - $2p$  mixing. The  $2s$ - $2p$  mixing can be calculated as a function of effective electric field on the H( $2s$ ) slow atom distribution which has a mean energy of 0.3 eV (see below). For a 50 G field the  $2s$ - $2p$  mixing has a calculated transition probability (Bethe & Salpeter 1977) of  $4.0 \times 10^2 \text{ s}^{-1}$  which gives the H atom a mean free path of 20 m, significantly larger than the distance to the chamber walls. In agreement with Vroom & de Heer (1969) we find a field of 50–100 G does not influence an H( $2p$ ) cross section measurement in a static gas experiment. The fast atom mean free path is 5 m, also significantly larger than the distance to the chamber walls.

### 3. CROSS SECTION FORMULATION

The data described here are fitted within experimental error using analytic cross sections having the form

$$\begin{aligned} \Omega_{ij}(X) = & C_0(1 - 1/X)(X^{-2}) \\ & + \sum_{k=1}^4 C_k(X - 1) \exp(-kC_8 X) \\ & + C_5 + \frac{C_6}{X} + C_7 \ln(X), \end{aligned} \quad (1)$$

where  $\Omega_{ij}(X)$  is the collision strength,  $X$  is the electron energy in threshold units, and the  $C_k$  are constants of the function (Shemansky *et al.* 1985a, b). The excitation cross section is given by the equation

$$\sigma_{ij}(X) = \Omega_{ij}(X)(E_{ij} X)^{-1}, \quad (2)$$

where  $\sigma_{ij}$  is the cross section in atomic units, and  $E_{ij}$  is the transition energy in rydberg units. Thermally averaged values and rate coefficients can be obtained from

$$\begin{aligned} \Omega_{ij}(T_e) = & \left\{ C_0[E_2(Y) - E_3(Y)] \right. \\ & + \left( C_6 + \frac{C_7}{Y} \right) E_1(Y) \left. \right\} Y \exp(Y) + C_5 \\ & + \sum_{k=1}^4 C_k \frac{Y}{(Y + kC_8)^2} \exp(-kC_8), \end{aligned} \quad (3)$$

where  $Y = E_{ij}/T_e$ ,  $T_e$  is electron temperature in rydbergs, and  $E_n(Y)$  is the exponential integral of order  $n$ . The rate coefficient ( $Q_{ij}$ ) in units of  $\text{cm}^3 \text{ s}^{-1}$  is given by

$$Q_{ij}(T_e) = (2.173 \times 10^{-8}) \left( \frac{Y}{E_{ij}} \right)^{1/2} \left[ \frac{\Omega_{ij}(T_e)}{\omega_i} \right] \exp(-Y). \quad (4)$$

### 4. RESULTS

The H Ly $\alpha$  excitation function from dissociative excitation of H<sub>2</sub> is shown in Figure 1. The absolute cross section from 14.7 eV to 700 eV is given in Table 1. The H Ly $\alpha$  excitation function was measured in four separate scans of 10–35 eV, 10–100 eV, 10–400 eV, and 10–700 eV. The energy step size varied from 0.029 eV to 0.391 eV. The former were at 0.1 nm spectral resolution and the latter two were at 0.5 nm spectral resolution. The 10–100 eV and 10–400 eV scans are shown in Figure 1, together with previous studies of H Ly $\alpha$  (Mumma & Zipf 1971; McLaughlin 1977). The low-energy structure at  $\approx 30$  eV was not clearly discernible in the excitation function shown by Mumma & Zipf (1971). McLaughlin (1977) shows structure at about the same energy of  $\sim 30$  eV. The agreement in shape between our data and those of Mumma & Zipf (1971) or McLaughlin (1977) shown in Figure 1 is excellent in the 50–400 eV region. We compare the measurements of the emission from H( $2p$ ) state with H $\alpha$  and H $\beta$  emission from the H( $3l$ ) and H( $4l$ ) states on a relative scale, based on measurements of Karolis & Harting (1978). There appears to be a systematic variation with principal quantum number of cross section ratio of the plateau structure(s) at 20–30 eV relative to the peak cross section at  $\approx 60$  eV.

It is not necessary to correct the measured signal at instrument bandpass of 0.1 nm for blending of the H<sub>2</sub> Lyman and Werner bands. The nearby bands are identified by Ajello *et al.* (1984). Previous publications have often failed to state the magnitude of the instrument bandpass. At lower resolution the H<sub>2</sub> bands blend with the H Ly $\alpha$  line. This problem is particularly important at thresholds where narrow Feshbach resonances contribute strongly to H<sub>2</sub> Lyman and Werner band excitation. Beyond 50 eV no correction is necessary; high (0.1 nm) and low (0.5 nm) spectral resolution give the same results.

The analytic excitation function model and experimental data from Figure 1 are shown in Figure 2. The data are a composite of the four cross section scans described above. The highest energy resolution data set is chosen for joining overlapping energy ranges. The agreement between data and model is better than 5%. The model includes a contribution from singlet and triplet states with a threshold of 14.7 eV, from triplet states at a threshold of 15.3 eV, and from singlet doubly excited states with thresholds  $\sim 30$  eV. The two singlet-state model cross sections consist of a dominant “slow” component and a weaker “fast” component. The singlet-state model for the “slow” component has an energy dependence described for the  $B'$  state. Because of the complexity of blended branches in the observed excitation function, we have analyzed the data by using the previously measured and analyzed shape function for the H<sub>2</sub>  $B'$  (Shemansky *et al.* 1985a) state as an established quantity to separate the slow dissociative component. Since this slow component is dominant (Fig. 2), the weaker components can be more accurately separated using the predetermined  $B'$  shape function. The sharp rise in the excitation function near threshold is apparently produced by a combination of exchange and resonance cross sections of triplet and singlet states. The excitation function in this region is fitted

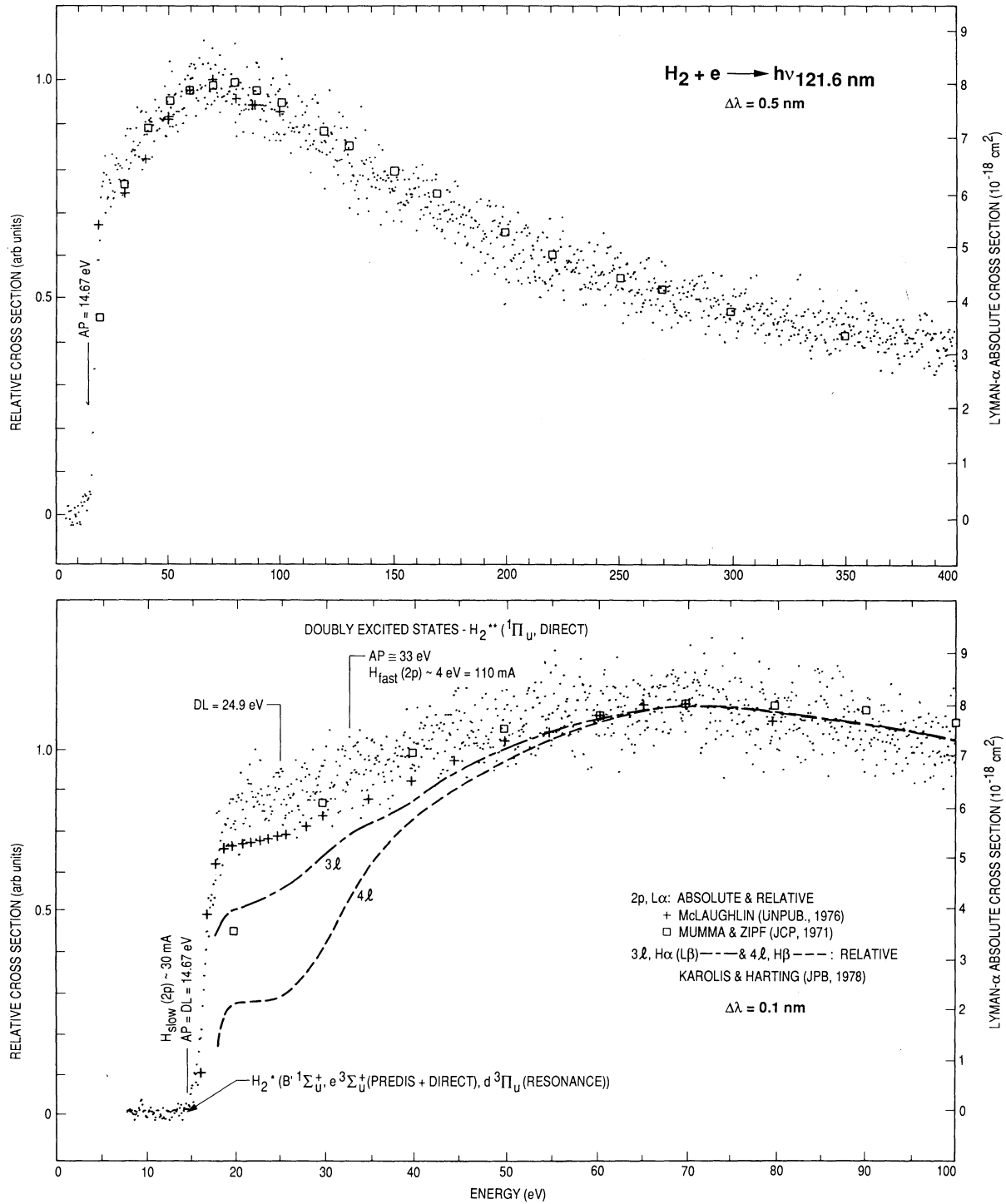


FIG. 1.—H Ly $\alpha$  measured excitation function (a) from 0 to 400 eV at a bandpass of 0.5 nm and (b) 0 to 100 eV at a bandpass of 0.1 nm. Data points were measured every 0.391 eV in (a) and every 0.0986 eV in (b). Important thresholds and data comparisons are indicated in the figure. The gas pressure was  $6 \times 10^{-6}$  torr.

with two exchange-type, sharply peaked cross sections and the dipole allowed  $H_2 B'$  contribution with thresholds at 14.7 and 15.3 eV (Fig. 3). The relative strengths of the three contributions to the cross section are determined by the fit to the measured cross sections from threshold to  $\sim 25$  eV. The shapes as well as magnitudes of the nondipole components are governed by the fitting process. A break in the slope of the excitation

function at 15.3 eV is visible in the data (Fig. 3) and allows the clear separation of the near-threshold excitation functions.

Triplet states make the major contribution to the emission cross section in the region between threshold and 25 eV. The rapid rise in cross section near threshold is indicative of the electron exchange processes. The model developed for the threshold region shows that the electron cross sections have

TABLE 1  
H Ly $\alpha$  CROSS SECTION FROM DISSOCIATIVE EXCITATION OF H $_2$

| ENERGY<br>(eV)<br>(1) | (2)  | (3)   | (4)  | (5)  | (6)  | (7)  | (8)  | (9)  |
|-----------------------|--|-------|------|------|------|------|------|------|
|                       | $\sigma[\text{H}(2p)] (10^{-18} \text{ cm}^2)$ |       |      |      |      |      |      |      |
| 14.92                 | 0.558  | 0.569 | 0.40 | 0.00 | 0.17 | 0.00 | 0.00 | 0.00 |
| 14.95                 | 0.719  | 0.632 | 0.44 | 0.00 | 0.19 | 0.00 | 0.00 | 0.00 |
| 14.98                 | 0.840  | 0.693 | 0.48 | 0.00 | 0.21 | 0.00 | 0.00 | 0.00 |
| 15.5                  | 1.62   | 1.94  | 1.06 | 0.30 | 0.54 | 0.00 | 0.00 | 0.00 |
| 16.0                  | 3.22   | 3.13  | 1.40 | 0.85 | 0.85 | 0.00 | 0.00 | 0.00 |
| 17.0                  | 4.72   | 4.65  | 1.68 | 1.55 | 1.41 | 0.00 | 0.00 | 0.00 |
| 18.0                  | 5.30   | 5.46  | 1.65 | 1.89 | 1.90 | 0.00 | 0.00 | 0.00 |
| 19.0                  | 5.79   | 5.85  | 1.48 | 2.35 | 2.35 | 0.00 | 0.00 | 0.00 |
| 20.0                  | 5.79   | 6.03  | 1.26 | 2.02 | 2.74 | 0.00 | 0.00 | 0.00 |
| 22.0                  | 5.47   | 6.09  | 0.83 | 1.85 | 3.41 | 0.00 | 0.00 | 0.00 |
| 24.0                  | 5.74   | 6.06  | 0.51 | 1.60 | 3.94 | 0.00 | 0.00 | 0.00 |
| 26.0                  | 6.27   | 6.04  | 0.31 | 1.35 | 4.37 | 0.01 | 0.00 | 0.00 |
| 30.0                  | 6.95   | 6.10  | 0.10 | 0.95 | 5.00 | 0.05 | 0.00 | 0.00 |
| 35.0                  | 6.83   | 6.77  | 0.02 | 0.63 | 5.48 | 0.07 | 0.48 | 0.09 |
| 40.0                  | 7.47   | 7.27  | 0.01 | 0.43 | 5.76 | 0.09 | 0.80 | 0.18 |
| 45.0                  | 7.37   | 7.61  | 0.00 | 0.31 | 5.91 | 0.11 | 1.04 | 0.24 |
| 50.0                  | 7.59   | 7.84  | 0.00 | 0.23 | 5.98 | 0.12 | 1.22 | 0.29 |
| 60.0                  | 8.52   | 8.05  | 0.00 | 0.14 | 5.97 | 0.13 | 1.46 | 0.36 |
| 70.0                  | 8.46   | 8.03  | 0.00 | 0.09 | 5.85 | 0.13 | 1.57 | 0.40 |
| 80.0                  | 7.59   | 7.86  | 0.00 | 0.06 | 5.68 | 0.12 | 1.59 | 0.41 |
| 90.0                  | 7.63   | 7.60  | 0.00 | 0.05 | 5.49 | 0.11 | 1.55 | 0.40 |
| 100.                  | 7.06   | 7.29  | 0.00 | 0.03 | 5.30 | 0.10 | 1.47 | 0.38 |
| 130.                  | 6.03   | 6.34  | 0.00 | 0.02 | 4.74 | 0.08 | 1.19 | 0.32 |
| 160.                  | 5.48   | 5.53  | 0.00 | 0.01 | 4.26 | 0.06 | 0.95 | 0.26 |
| 200.                  | 4.72   | 4.77  | 0.00 | 0.00 | 3.74 | 0.05 | 0.77 | 0.20 |
| 250.                  | 4.18   | 4.12  | 0.00 | 0.00 | 3.24 | 0.05 | 0.66 | 0.17 |
| 300.                  | 3.89   | 3.67  | 0.00 | 0.00 | 2.87 | 0.04 | 0.60 | 0.16 |
| 400.                  | 3.11   | 3.05  | 0.00 | 0.00 | 2.35 | 0.04 | 0.53 | 0.14 |
| 500.                  | 2.36   | 2.62  | 0.00 | 0.00 | 2.00 | 0.03 | 0.46 | 0.12 |
| 600.                  | 2.25   | 2.30  | 0.00 | 0.00 | 1.76 | 0.03 | 0.40 | 0.11 |
| 700.                  | 1.95   | 2.05  | 0.00 | 0.00 | 1.58 | 0.02 | 0.36 | 0.09 |
| 1000.                 | ...  | 1.56  | 0.00 | 0.00 | 1.22 | 0.02 | 0.26 | 0.07 |
| 1500.                 | ...  | 1.13  | 0.00 | 0.00 | 0.90 | 0.01 | 0.17 | 0.05 |
| 2000.                 | ...  | 0.90  | 0.00 | 0.00 | 0.72 | 0.01 | 0.13 | 0.03 |
| 2500.                 | ...  | 0.75  | 0.00 | 0.00 | 0.61 | 0.01 | 0.10 | 0.03 |
| 3000.                 | ...  | 0.64  | 0.00 | 0.00 | 0.53 | 0.01 | 0.09 | 0.02 |
| 4000.                 | ...  | 0.51  | 0.00 | 0.00 | 0.42 | 0.00 | 0.07 | 0.02 |
| 5000.                 | ...  | 0.42  | 0.00 | 0.00 | 0.35 | 0.00 | 0.05 | 0.01 |
| 6000.                 | ...  | 0.36  | 0.00 | 0.00 | 0.30 | 0.00 | 0.04 | 0.01 |
| 8000.                 | ...  | 0.28  | 0.00 | 0.00 | 0.24 | 0.00 | 0.03 | 0.01 |
| 10,000.               | ...  | 0.24  | 0.00 | 0.00 | 0.20 | 0.00 | 0.03 | 0.01 |

COLLISION STRENGTH COEFFICIENTS FOR  $e + \text{H}_2 \rightarrow \text{H Ly}\alpha$

| $i$ | $E_{ij}$ | $C_0$      | $C_1$       | $C_2$      | $C_3$      | $C_4$       | $C_5$       | $C_6$       | $C_7$      | $C_8$      |
|-----|----------|------------|-------------|------------|------------|-------------|-------------|-------------|------------|------------|
| 1   | 14.67    | 0.0000E+00 | 3.3734E+01  | 0.0000E+00 | 0.0000E+00 | 0.0000E+00  | 0.0000E+00  | 0.0000E+00  | 0.0000E+00 | 4.6700E+00 |
| 2   | 15.28    | 1.4251E-01 | 1.4462E+00  | 1.5436E+01 | 0.0000E+00 | 0.0000E+00  | 0.0000E+00  | 0.0000E+00  | 0.0000E+00 | 2.8184E+00 |
| 3   | 14.67    | 0.0000E+00 | 1.9290E-02  | 0.0000E+00 | 0.0000E+00 | -2.5192E-02 | -1.5573E-01 | 1.5573E-01  | 2.7758E-01 | 1.2589E-01 |
| 4   | 24.90    | 1.7840E-03 | -5.2230E-03 | 0.0000E+00 | 5.2390E-02 | -8.5225E-02 | 1.4749E-02  | -1.4749E-02 | 0.0000E+00 | 2.6303E-01 |
| 5   | 30.20    | 2.6760E-02 | -7.8345E-02 | 0.0000E+00 | 7.8585E-01 | -1.2784E+00 | 2.2123E-01  | -2.2123E-01 | 0.0000E+00 | 2.6303E-01 |
| 6   | 31.50    | 7.1360E-03 | -2.0892E-02 | 0.0000E+00 | 2.0956E-01 | -3.4090E-01 | 5.8994E-02  | -5.8994E-02 | 0.0000E+00 | 2.6303E-01 |

Col. (2)—Present measurements; smoothed data of Figs. 1 and 2; (3) model calculation of total H(2p) cross section; sum of components  $i = 1-6$ ; (4) electron exchange and resonance contributions with threshold  $E_{ij} = 14.67$  eV; component  $i = 1$ ; (5) electron exchange and resonance contributions with threshold  $E_{ij} = 15.28$  eV; component  $i = 2$ ; (6) electric dipole contribution with threshold  $E_{ij} = 14.67$  eV; component  $i = 3$ ; (7)-(9) doubly excited state contributions with thresholds  $E_{ij} = 24.9-31.5$  eV; components  $i = 4-6$ .

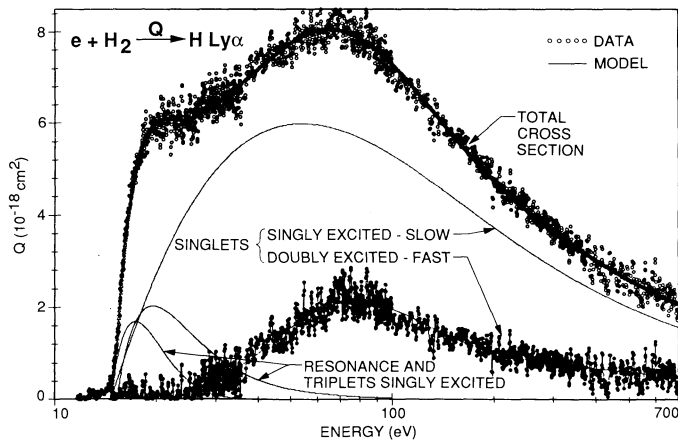


FIG. 2.—Excitation function of H Ly $\alpha$  from dissociative excitation of H $_2$ . Modified Born approximation model (solid line) compared to data (dots). The constants for the model (Shemansky 1985a, b) are given in Table 1. The plot also shows the decomposition of the model into the major components—electric dipole (slow atoms), triplets (slow atoms), and both model and data residue for dissociation of doubly excited states (fast atoms).

two or more branches of FWHM of about 5 and 10 eV, respectively. The cross sections are attributed to a combination of resonance excitation of the  $d^3\Pi_u$  state, followed by predissociation by the  $e^3\Sigma_u^+$  state and direct dissociation of the  $e^3\Sigma_u^+$  state. The electron energy resolution of 0.3 eV does not allow a separation of the narrow ( $\leq 40$  meV), short-lived ( $\tau \approx 10^{-14}$  s) resonance states of H $_2^+$  (Weingartshofer et al. 1970, 1975) which are separated by  $\approx 0.1$ –0.2 eV. Instead we measure a convolution of the resonance and direct electron exchange processes. The inflection at 15.3 eV is probably indicative of the resonance processes. The cross sections for resonance processes and triplet state excitation have peak values in the range 15–20 eV (Table 1). The difference between the modeled excitation function established by fitting the data up to 25 eV as described above and the measured data is shown in Figure 2. The residue shows a slowly rising cross section from 25 to 30 eV to a peak near 80 eV with a value  $\sigma(80 \text{ eV}) \sim 2 \times 10^{-18} \text{ cm}^2$ . The residue has been fitted with a combination of three excitation functions having identical shape functions but with thresholds  $E_{ij} = 24.9, 30.2,$  and  $31.5$  eV, corresponding to the major doubly excited states (Guberman 1983). The division of

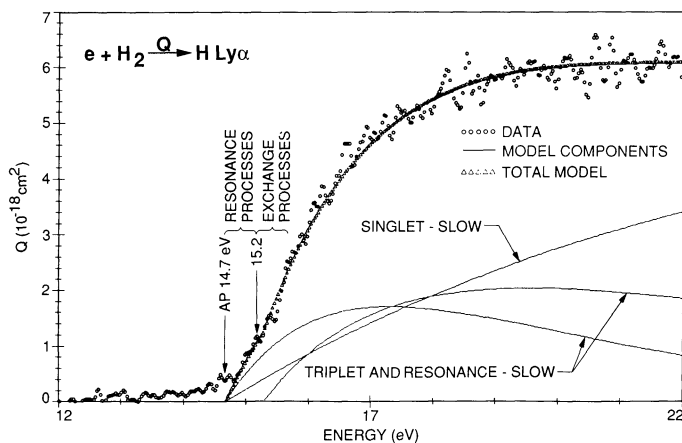


FIG. 3.—Comparison of experimental excitation function with analytic model in the threshold region. The instrumental bandpass was 0.1 nm. Data points were measured every 0.029 eV.

strength between these three states is very uncertain in this reduction and only the total has a well-determined value.

The smoothed data values are given in Table 1 from threshold to 700 eV, along with the model values and the collision strength parameters determined in the fitting process. The results obtained here can be compared to the Vroom & de Heer (1969) data (50 eV–6 keV) for the purpose of obtaining a verification of the predicted cross section at high energy. Figure 4 shows the collision strength calculated with the present model compared to the Vroom & de Heer (1969) data normalized, in absolute value, at 100 eV. The predicted values fall within measurement error over the entire range of the data. Above 1 keV the model and the Vroom & de Heer (1969) data follow the asymptotic Born dipole shape, dominated by the singlet-state dipole component.

The decomposition of the H Ly $\alpha$  excitation function in the present analysis provides the critical information needed to determine the partitioning of the remaining dissociation fragments produced by electron impact on H $_2$ , and hence the total neutral dissociation cross section. As we discuss further below, the partitioning of H(2p) and H(2s) fragments in the dissociation process is essentially inaccessible to theoretical calculation. We infer the H(2s) cross section in the following way. The electric dipole component of the H(2p) cross section is  $5.3 \times 10^{-18} \text{ cm}^2$  at 100 eV, determined from the analytic data in Table 1. This cross section is composed of the total predissociation of the H $_2$  Rydberg states, direct dissociation, and cascade from the states producing H( $>2l$ ) atoms. The predissociation cross sections of the H $_2$  Rydberg states  $B', B'', D,$  and  $D'$  have been obtained by Ajello et al. (1988). Glass-Maujean, Frohlich, & Beswick (1986) have obtained a measure of the direct/predissociation ratio. This combination gives the information required to obtain the total electric dipole H(2l) cross section. The relatively small cascade cross section can be obtained from the measured H $\alpha$  and H $\beta$  cross sections. Assuming that higher Rydberg states make a negligible contribution of H(2l), the total H(2l) electric dipole cross section is  $8.79 \times 10^{-18} \text{ cm}^2$ . The excess over the H(2p) cross section,  $3.51 \times 10^{-18} \text{ cm}^2$ , is the H(2s) cross section, as shown in Table 2. The doubly excited state cross section at 100 eV is  $3.04 \times 10^{-18} \text{ cm}^2$ , according to Table 2, and is equally divided in H(2p) and H(2s) fragments. The small cascade contribution

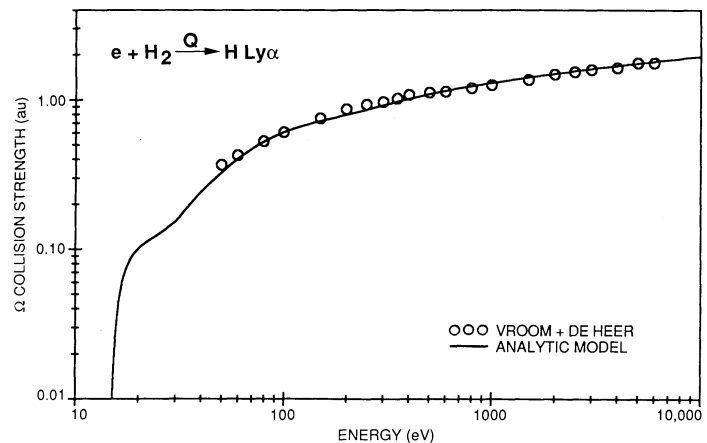


FIG. 4.—Collision strength of H Ly $\alpha$  emission cross section from dissociative excitation of H $_2$  plotted against energy. The Vroom & de Heer (1969) data are overplotted on the model as circles, normalized for the present collision strength value at 100 eV.

TABLE 2  
ELECTRON DISSOCIATIVE EXCITATION PARTITIONING  
OF H(2*p*, 2*s*, 1*s*) STATES AT 100 eV (10<sup>-18</sup> cm<sup>2</sup>)

| Source                                    | 2 <i>l</i>        | 2 <i>p</i>        | 2 <i>s</i>        | 1 <i>s</i> |
|---|-------------------|-------------------|-------------------|------------|
| Singly excited states:                    |                   |                   |                   |            |
| H <sub>2</sub> B''                        | 2.40 <sup>a</sup> | ...               | ...               | 2.40       |
| H <sub>2</sub> D                          | 2.00 <sup>a</sup> | ...               | ...               | 2.00       |
| H <sub>2</sub> D'                         | 1.50 <sup>a</sup> | ...               | ...               | 1.50       |
| Total predissociation                     | 5.90              | ...               | ...               | 5.90       |
| H <sub>2</sub> B' (direct dissociation)   | 1.93              | ...               | ...               | 1.93       |
| H <sub>2</sub> B, C (direct dissociation) | 0.59 <sup>b</sup> | 0.59              | 0.00              | 0.59       |
| Total direct dissociation                 | 2.52 <sup>b</sup> | ...               | ...               | 2.52       |
| Subtotal                                  | 8.42              | 4.94              | 3.48              | 8.42       |
| Cascade                                   | 0.37 <sup>c</sup> | 0.34 <sup>c</sup> | 0.03 <sup>c</sup> | 0.69       |
| Total (<0.5 eV/atom)                      | 8.79              | 5.32              | 3.51              | 9.11       |
| Doubly excited states:                    |                   |                   |                   |            |
| Subtotal                                  | 3.04              | 1.52              | 1.52              | ...        |
| Cascade                                   | 0.56              | 0.50              | 0.06              | 0.49       |
| Total (>0.5 eV)                           | 3.60              | 2.02              | 1.58              | 0.49       |
| Total excited states                      | 12.39             | 7.30              | 5.09              | 9.60       |

<sup>a</sup> Ajello et al. 1988.

<sup>b</sup> Glass-Maujean et al. 1986, 1988.

<sup>c</sup> Ajello et al. 1984; Karolis & Harting 1978; Higo & Ogawa 1980.

from higher doubly excited states can be estimated from the Karolis & Harting (1978) data, giving a total H(2*l*) cross section of  $12.4 \times 10^{-18}$  cm<sup>2</sup>. The details of the atomic fragment budget are given in Table 2. The total H atom cross section is then  $22 \times 10^{-18}$  cm<sup>2</sup> with the inclusion of the H(1*s*) fragments (Table 2).

## 5. DISCUSSION

It is well known that there are two distinct groups of energy distributions of atoms formed on dissociative excitation of H<sub>2</sub>. These groups are referred to as "fast" and "slow," with energy peaks at  $\approx 4$  and  $\approx 0.3$  eV, respectively. The dissociation limits (DL) and AP are indicated in Figure 1 for both distributions. The most recent works with a complete review of the history of the subject are by Compton & Bardsley (1984), Landau, Hall, & Pichou (1981), and Zipf (1984). Previous experiments on direct H(2*l*) production by electrons have studied H(2*s*) formation in (1) time of flight measurements produced by electron impact (Leventhal, Robiscoe, & Lea 1967; Spezeski, Kalman, & McIntyre 1980), (2) angular distribution measurements of H fragments (Misakian & Zorn 1972), (3) UV emission studies by quenching H(2*s*) state with an electric field (Vroom & de Heer 1969). Research on H(2*p*) over a range of electron impact energies from 11 eV to 6 keV has been published by Vroom & de Heer (1969), Mumma & Zipf (1971), and Böse & Linder (1979). Cascade production of H(2*p*) and H(2*s*) has been estimated by observing H $\alpha$  and H $\beta$  emissions. The most recent example is the excitation function measurements by Karolis & Harting (1978) normalized to data of Vroom & de Heer (1969). Another important work on H $\alpha$  and H $\beta$  was by Khayrallah (1976). The most detailed research of H(2*s*, 2*p*) slow atom production from photodissociation of H<sub>2</sub> is by Glass-Maujean and coworkers using synchrotron radiation from a storage ring (Glass-Maujean, Guyon, & Breton 1986; Glass-Maujean *et al.*, 1988; Glass-Maujean 1989; Beswick & Glass-Maujean 1987). Glass-Maujean *et al.* (1986, 1988) obtained the H(2*s*, 2*p*) yield relative to H(2*l*) at selected photon energies in the direct dissociation continuum from 14.8 to 15.0 eV and the partitioning of H(2*l*) between direct dissociation and predissociation by integrating the respective cross sections from 14.6 to 16.1 eV. All experiments show that the Balmer lines are excited by both predissociation and direct dissociation by bound states with electronic levels below 25 eV. At  $\sim 25$  eV structure is observed for the production of Balmer lines from new thresholds marking the AP of doubly excited states for the major dissociative channel. The related cross section for H Ly $\beta$  has been measured by Ajello *et al.* (1984) and shows good agreement with the H $\alpha$  measurements.

The dissociation cross section budget.—Previous electron impact experiments have shown that doubly excited states, principally the Q<sub>2</sub> state that dissociates into H(2*s*) and H(2*p*) were responsible for the fast metastables (Spezeski, Kalman, & McIntyre 1980). The slow H(2*s*) atoms arise from transitions to singly excited states above the H(1*s*) + H(2*s*) limit and likewise for the H(2*p*) atoms. A simplified potential energy diagram (Sharp 1971) with the Franck-Condon region for H<sub>2</sub> is shown in Figure 5. The Franck-Condon region encloses portions of the excited potential curves containing the asymptotic DL; slow H(2*s*) and H(2*p*) atoms should be produced with high probability. The sharp AP of 14.7 eV in Figure 1 at the DL corresponds to this case. From the myriad manifold of states that can be excited by low-energy electrons near the AP only the B'<sup>1</sup> $\Sigma_u^+$ , e<sup>3</sup> $\Sigma_u^+$ , H<sup>1</sup> $\Sigma_g^+$ , and h<sup>3</sup> $\Sigma_g^+$  states have repulsive portions of the potential curve in the Franck-Condon region. The first two of these states in the separated atom limit adiabatic approximation correlate to H(1*s*) + H(2*s*) atoms. However, the nonadiabatic coupling of these curves at large internuclear distances will determine the fraction of H(2*s*) atoms that cross to H(2*p*). Beswick & Glass-Maujean (1987) have shown that interference effects between the two dissociative states B and B' can lead to crossover of H(2*p*) and H(2*s*) fragments. Theory at this stage shows only qualitative agreement with experiment (Glass-Maujean *et al.* 1988). The experimentally measured yield in the direct dissociation continuum is found to be a sharp function of excess energy. In this regard Glass-Maujean *et al.* (1988) have measured the H(2*p*) and H(2*s*) branching ratio at six energies in the direct photodissociation continuum and at one energy at a D state predissociation peak. The H<sup>1</sup> $\Sigma_g^+$  state is the only singlet state in the Franck-Condon region that correlates to H(1*s*) + H(2*p*). It is an optically forbidden transition. The B and C states, on the other hand, are only weakly dissociated relative to direct excitation to bound levels but have been shown to contribute about 23% to the direct H(2*l*) continuum (Glass-Maujean *et al.* 1986). The C state has a larger direct dissociation cross section and is assumed to be dominant in Table 2.

According to photodissociation experiments by Glass-Maujean *et al.* (1986) the B' state is the strongest contributor to direct dissociation. The electric dipole component of the H(2*p*) cross section in the present analysis is  $5.3 \times 10^{-18}$  cm<sup>2</sup> at 100 eV. This cross section is determined by the singlet-state Rydberg series predissociation and direct dissociation branches. Table 2 shows the decomposition of the dissociation cross section. The present experiment provides a measure of only the H(2*p*) production rate. However, the H(2*l*) predissociation cross sections for the B'', D, and D' states have been obtained by Ajello *et al.* (1988), and these quantities can be used with the relative rates estimated by Glass-Maujean *et al.* (1986) to place the singlet-state electric dipole cross sections for the total of predissociation and direct dissociation on an absolute scale. The difference between the H(2*l*) cross section and the value obtained for H(2*p*) then provides a determination of the slow component of the H(2*s*) and H(1*s*) excitation cross sections. The cross sections for the singly excited state contribution estimated in this way are shown in Table 2. For energies

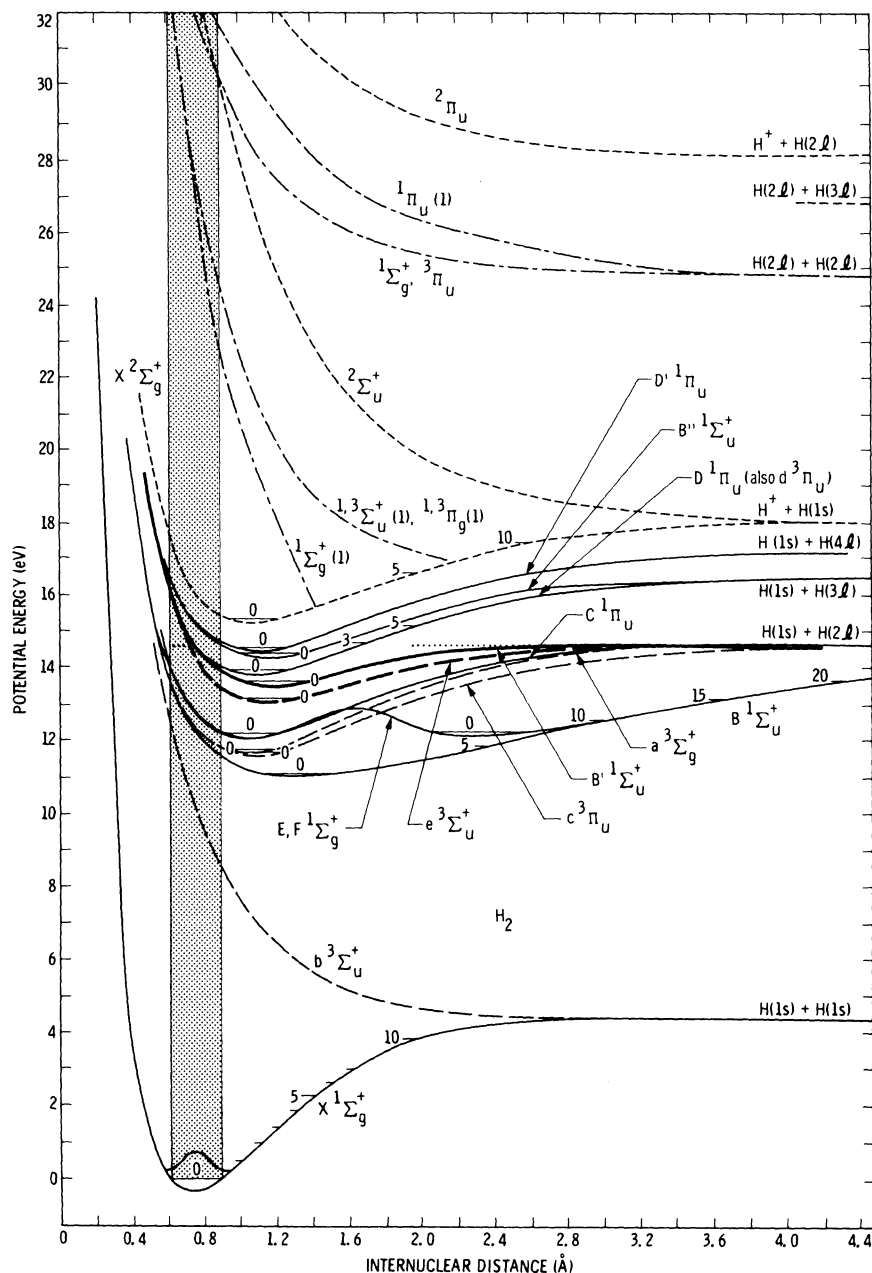


FIG. 5.—Simplified potential energy diagram of  $H_2$  with the most important states relevant to this study indicated. The singly excited states are taken from Sharp (1971) and the doubly excited states are taken from Guberman (1983). Singlet states of  $H_2$  are solid line, triplet states are long dash,  $H_2^+$  states are short dash, and doubly excited states are long dash, short dash. The Franck-Condon region is shaded and the  $e$  and  $B'$  states are shown in bold.

above 50 eV the  $H(2p)/H(2l)$  yield from electron impact experiments of Vroom & de Heer (1969) is 67%, and in the present experiment, 59%. On the other hand, in the energy range from 0 to 1.5 eV above threshold Glass-Maujean et al. (1986) have obtained a 34%  $H(2p)/H(2l)$  yield from photodissociation experiments. The Glass-Maujean et al. (1968) experiment, which detects both  $H(2p)$  and  $H(2s)$  slow atoms arising from optically allowed states, attributes 90% of the observed dissociation and predissociation to the  $B'$  state. The remaining 10% mostly arise from direct dissociation of the  $B$  and  $C$  continua. In total, predissociation contributes 70% and direct dissociation 30% to the  $H(2l)$  yield. The yield is obtained by integrating the photodissociation cross sections from 14.6 to 16.1 eV for white light incident on the molecule. This is the energy

range of interest for electron impact experiments at high energy (preferably a factor of 10 above threshold) where an electron impact experiment approximates conditions of a photon impact absorption experiment. The Franck-Condon region for the continua of the  $B'$ ,  $B$ , and  $C$  states shown in Figure 5 spans the energy range from 14.67 to 17 eV, the energy range considered in the calculation of dissociation yields (Glass-Maujean et al. 1986). Most of the dissociation occurs for transitions in the energy range from 14.67 eV to the ionization limit at 15.5 eV. The vibrational overlap integral for the two types of experiments measuring direct and predissociation processes are the same. The high electron impact energy ensures the first term of the Born approximation is the dominant term. In the Born region the ratio of direct and predissocia-

tion yields is nearly identical for the two types of experiments. This is the critical assumption in our calculation using the experimental data at 100 eV (actually only a factor 7 above threshold energy) to determine the branching of H(2s, 2p). The primary states in the production of slow atoms by predissociation are the *D*, *B'*, and *D'* states mixing with *B'* state (Guyon, Breton, & Glass-Maujean 1979).

The technique in the Glass-Maujean et al. (1986) experiment involved a quenching electric field to induce and measure a 2s–2p transition at a pressure of  $2 \times 10^{-3}$  torr. The high pressure in this experiment is a severe disadvantage because of strong collisional quenching of the H(2s) atoms. The partitioning of H(2s and 2p) atoms from photodissociation (Glass-Maujean et al. 1988) in the range 0–0.2 eV above threshold varies by a factor of 2 with excess energy above 14.67 eV. For photon absorption at wavelengths above 84.2 nm the H(2p)/H(2l) yield is dominant and for wavelengths between 83.7 nm and 84.2 nm the H(2s)/H(2l) branch is dominant. The experimental measurement is a demonstration of the interference effects on the H(2s, 2p) partitioning from simultaneous excitation of two dissociative excitation continua (*B*, *B'*). In non-adiabatic approximation theory these two states are coupled together at large internuclear distance. The H(2p) + H(1s) state can be produced by direct excitation and predissociation into the *B* state (adiabatic process) or direct excitation into the *B'* state followed by transition to the *B* state (nonadiabatic process). Thus the *B* state contributes to both H(2s) and H(2p) production with yields relative to H(2l) of 43% and 57% respectively, on the average in the classical limit neglecting interference effects (Glass-Maujean et al. 1986). In the closed *B*–*B'* system the *B'* state yield must then be 57% for H(2s) production and 43% for H(2p) production. The direct dissociation continuum of the *C* state has a yield H(2p)/H(2l) = 100%. The *C* state as mentioned earlier contributes to the direct dissociation continuum but does not interact with the *B'* state. If we were to use these yields on the singly excited states in Table 2, the combined effects of predissociation and direct dissociation on the branching ratio would be expected to produce slightly more H(2s) atoms. In fact the analysis of the electron impact experiment obtains slightly more H(2p) than H(2s) atoms. The electron impact experiments measure the combined effects on the branching ratio of both direct and predissociation. On the other hand, the photon impact experiments that provide the ability to separate the processes study only a limited energy range and should not be compared directly to the electron impact experiment performed here. The electron impact experiment measures the branching ratio over the integrated width of the Franck-Condon region. This energy range extends to approximately 1.7 eV above threshold.

In the present electron impact experiment H(2p) production proceeds from optically allowed singlet states as in the photodissociation study, but in addition, optically forbidden triplet transitions are produced. Indeed, the sharp rise at threshold is probably due to resonance excitation of the *d* state followed by predissociation by the *e* state. In addition, direct dissociation by electron exchange to the *e* and *h* states may be important in the formation of slow H(2s, 2p) atoms above the resonance energies. Two states that are important in production of H<sub>2</sub> molecular emissions are the  $a^3\Sigma_g^+$  and  $c^3\Pi_u$  states. The  $a^3\Sigma_g^+$  and  $c^3\Pi_u$  have their continua outside the Franck-Condon overlap region and do not contribute to the direct cross section.

Direct evidence for H(2p) + H(1s) production from triplet

states can be found in the electron-photon coincidence measurements of Böse & Linder (1979). Their measured threshold of 14.7 eV is attributed to predissociation of the  $d^3\Pi_u(v > 4)$  state by the  $e^3\Sigma_u^+$  state. Spectroscopic evidence exists for this predissociation (Dieke 1935). It is probable that the threshold cross section of the *d* state vibrational levels which have large and sharp excitation cross sections from Feshbach resonances observed at 20 meV resolution by Weingartshofer et al. (1970, 1975) contribute more strongly than do direct exchange processes. Strong threshold peaks for  $v' = 4, 5, 6$  seem to have been observed by Weingartshofer et al. at 14.876, 15.094, 15.298 eV up to 16 eV, respectively. The importance of resonances in the H Ly $\alpha$  dissociative excitation process is found in the inflection in the cross section at  $\approx 15.3$  eV. Resonances seem to dominate all the VUV emission data for singlet and triplet state molecular emission as well in this energy region for the first 1 or 2 eV above threshold. The results will be described in another paper in preparation.

The most complete set of calculations involving 24 doubly excited autoionizing states of H<sub>2</sub> is given by Guberman (1983). Evidence for the importance of doubly excited states in the excitation function of H Ly $\alpha$  in Figure 1 arises from the AP observed at 32 eV, which is 7 eV above the 24.9 eV H(2p) + H(2s) DL. The small 20% increase in absolute cross section from 30 to 60 eV indicates that doubly excited states contribute a small fraction of the total cross section. The Guberman (1983) calculation of  $Q_2$  states (Fig. 5) having an H<sub>2</sub><sup>+</sup> ( $^2\Pi_u$  core) show a whole manifold of repulsive states converging to the H(2p) + H(2s) dissociation limit. Selection rules  $\Delta\Lambda = 0, \pm 1, \Sigma^+ \leftrightarrow \Sigma^-, g \leftrightarrow u$ , and  $\Delta S = 0$  suggest that  $^1\Pi_u$  and  $^1\Sigma_g^+$  states contribute to the dissociation. Calculations show the first two  $^1\Sigma_g^+, ^1\Pi_u$  states have thresholds at the large internuclear distance limit of the Franck-Condon region in Figure 5 of 30.2 and 31.5 eV, respectively. These states lie above the 24.9 eV dissociation limit and account for the origin of the fast H(2p, 2s) atoms.

The doubly excited state decays through autoionization (H<sub>2</sub><sup>+</sup> + *e* or H<sup>+</sup> + H<sup>−</sup>) stabilization and dissociation [H(2p) + H(2s)]. There may be a small contribution to the dissociative cross section from  $Q_1$  states (states with H<sub>2</sub><sup>+</sup>  $^2\Sigma_u^+$  ion core shown in Fig. 5) which are strongly autoionized (80%–95%) at energies below the 29 eV threshold for the  $Q_2$  states (Misakian and Zorn 1972). Spezeski et al. (1980) observe fast H(2s) fragments at 27 eV with a maximum kinetic energy of 2.7 eV atom<sup>−1</sup>. The candidate  $Q_1$  states contributing to this process with the threshold energies (23.0–28.2 eV) are given in Guberman (1983). For example,  $Q_1^1\Sigma_g^+(1)$  and  $Q_1^1\Sigma_g^+(2)$  with thresholds at 23.0 and 27.2 eV are possible states.  $Q_1$  states appear to be more important for the 3l and 4l production. Evidence of this fact is the large cross section increase at the  $24 \pm 1$  eV threshold for H $\alpha$  (and probably H Ly $\beta$ ) and H $\beta$  (Karolis & Harting 1978; Higo & Ogawa 1980). The first doubly excited state  $Q_1^1\Sigma_g^+(1)$  undoubtedly contributes to the H $\alpha$  and H $\beta$  emission and is more important on a relative basis than for H Ly $\alpha$ .

We estimate the H(2s) cross section and yield using the measurement of H(2p) emission cross section in this paper and the H(2l) predissociation cross section analysis from previous results (Ajello et al. 1988). The branching of H(2s, 2p) from various singly and doubly excited processes is shown in Table 2 at 100 eV. The predissociation cross section for each state is given by Ajello et al. (1988) and is transcribed in Table 2 under the 2l column for singly excited states. Direct excitation of the

$B'$ ,  $B$ , and  $C$  dissociation continua are the second most important processes. Cascade to  $2p$  from the  $3l$  and  $4l$  levels is a minor contribution to the total direct excitation by singly excited states. The excitation rates of the  $3l$  level leading to cascade to the  $2p$  and direct transition to the  $1s$  level has been discussed by Ajello et al. (1984). The present calculations make use of the  $H\alpha$  ( $3l-2l$ ) absolute cross section ( $\sigma = 9.3 \times 10^{-19}$  cm<sup>2</sup>) and  $H\beta$  cross section energy dependence (Fig. 1) measured by Karolis & Harting (1978). The  $H\beta$  line shape of Higo & Ogawa (1980) clearly separates fast and slow atom  $4l-2l$  emission-line profile intensities. Integrating over the Higo & Ogawa (1990) line we find 20% slow, 80% fast  $4l$  atoms at 100 eV. The  $H$  Ly $\beta$  ( $3p-1s$ ) cross section is  $5.5 \times 10^{-19}$  cm<sup>2</sup> from Ajello et al. (1984), scaled by the Ajello et al. (1988) data. The cascade quantities are indicated in Table 2 for both the doubly and singly excited states. The doubly excited states contribute a total of about 29% of the  $2l$  cross sections at 100 eV based on the modeled contribution of the process with  $AP \approx 30$  eV. The  $2s$  and  $2p$  yields are assumed to be in a ratio of 1 for the doubly excited states. The exact disposition of  $2s$ ,  $2p$  branching from the doubly excited states is very difficult to calculate because of the competition for the stabilization of the  $Q_1$  states between ionization and formation of excited Rydberg states. A statistical argument for the dissociation of the  $Q_2$  states suggests that formation of  $2p$  is slightly more likely than  $2s$  formation (Guberman 1983). The present results are basically in agreement with Vroom & de Heer (1969) within experimental uncertainties. The uncertainty in cross section values in the present experiment are estimated to be a root sum square error of the following principal sources: (1) 8% error in  $H$  Ly $\alpha$  absolute cross section at 100 eV, (2) 10% uncertainty in the ratio of direct to predissociation cross sections at 100 eV, (3) 10% error in the absolute predissociation  $2l$  cross section from Ajello et al. (1988), (4) additional 5% error from other sources, for instance, the branching of doubly excited states. The root sum square uncertainty is 17%. We have reviewed the sources of the  $H$  Ly $\alpha$  cross section in item (1) above in Pang et al. (1987). In a more recent review, van der Burgt, Westerveld, & Risley (1989) have found the same result for the unweighted average of the four different methods of obtaining the  $H$  Ly $\alpha$  cross section. All of the results are in the overlap region of  $1 \sigma$  error bars. The narrowness of these gives an uncertainty of 8%. However, an unsatisfactory aspect of this result is the value ( $8.2 \pm 1.2 \times 10^{-18}$  cm<sup>2</sup>) obtained by Shemansky et al. (1985a), based on the cross section of the  $H_2$  bands as a benchmark relative to the  $H$  Ly $\alpha$  line. The oscillator strengths of the bands to which the band cross sections are referenced have a claimed uncertainty of  $\sim 2\%$ . Although the  $H$  Ly $\alpha$  cross section values lie within estimated error bars the discrepancy seems rather large (we continue to obtain the same value with different experimental spectra, tending to eliminate statistical or experimental aberration), and we have been unable to identify possible sources of systematic error. This issue requires further investigation. The uncertainty reported in the Vroom & de Heer (1969) measurement of  $H(2s, 2p)$  yield is  $\sim 15\%$ . We expect a photodissociation  $H(2s, 2p)$  yield experiment extended to all photon energies from 14 to 17 eV and averaged with photon energy over both direct and predissociation processes would show a similar result.

The difference in the cross section for production of the "slow" (singly excited) and "fast" (doubly excited)  $H(2s)$  atoms is in qualitative agreement with time of flight studies of  $H(2s)$  atoms (Spezeski et al. 1980; Leventhal et al. 1967).

These studies found the yield of "fast"  $H$  fragments to be about one order of magnitude less than for the "slow" fragments at all energies studied from 15 to 100 eV. The exact ratio varies with energy as can be seen from published time-of-flight spectra. The electric dipole cross sections do not become dominant until 30 eV. This interpretation of  $H(2p)$  emission cross section data is consistent with the time-of-flight experiments (Spezeski et al. 1980; Leventhal et al. 1967) and angular distribution of atomic fragments (Misakian & Zorn 1972). The similarities in cross section structure for  $H(2s)$  and  $H(2p)$  are also strong evidence for thorough mixing of the asymptotic  $2s$  and  $2p$  dissociation channels. From an experimental point of view the cross section measured in our study near the DL shown in Figure 1 is in good agreement with that published by Mumma & Zipf (1971) (see Fig. 1). Our cross section is about 10% larger with proper updating of their result based on the revised  $H$  Ly $\alpha$  cross section. These differences are not understood. The pressure in the present experiment was two orders of magnitude lower than the experiments of Mumma & Zipf (1971) and McLaughlin (1977) and is a major experimental advantage for elimination of secondary pressure effects such as  $2s$  quenching to the  $2p$  state. Future emission cross section studies with a high-resolution ( $\approx 50$  meV) electron gun are warranted in the threshold region to study the Feshbach resonances and separate the direct and resonance  $2p$  components.

## 6. SUMMARY

We have measured the excitation function of  $H$  Ly $\alpha$  from the dissociation of electron excited  $H_2$  over the range 10–700 eV. The process is astrophysically important and is an emission feature often used as a calibration standard in the UV (Shemansky et al. 1985a, b; Ajello & Franklin 1985; Pang et al. 1987). The excitation function has been partitioned into six components, representing contributions from resonance, triplet, singlet, and doubly excited states. The decomposition was accomplished primarily by utilizing the accurately known shape of the dominant singlet-state electric dipole contributions, determined from measurements of the excitation of the  $H_2$  Rydberg bands that form the source of this  $H(2p)$  component. The contributions of the components to the total are shown in Table 1, normalized to  $\sigma[H(2p)] = 7.3 \times 10^{-18}$  cm<sup>2</sup> at 100 eV. The analysis predicts the cross section to energies higher than the present experimental limit, and we find that the predicted shape is in close agreement with the measurements of Vroom & de Heer (1969) over the range 50 eV–6 keV. At 6 keV the cross section is dominated by the electric dipole first Born component, while at 100 eV the electric dipole component constitutes 73% of the total  $H(2p)$  cross section.

The reduction of the  $H(2p)$  excitation function shown in Table 1 combined with published  $H_2$  band cross sections (Ajello et al. 1988), an estimate of the ratio of predissociation to direct dissociation (Glass-Maujean et al. 1986), and the contribution of the higher atomic Rydberg states, have allowed the calculation of the cross sections of the  $H(2s)$  and  $H(1s)$  components. The total dissociation cross section at 100 eV is  $\sigma[H(nl)] = 22 \times 10^{-18}$  cm<sup>2</sup>, containing  $\sigma[H(2s)] = 5.1 \times 10^{-18}$  cm<sup>2</sup> and  $\sigma[H(1s)] = 9.6 \times 10^{-18}$  cm<sup>2</sup> in  $H(2s)$  and  $H(1s)$  components. The uncertainties in these quantities have been discussed above.

Discussions with M. Glass-Maujean and S. Guberman are gratefully acknowledged. This work was supported by the Air

Force Office of Scientific Research (AFOSR), the Aeronomy Program of the National Science Foundation (grant number ATM 8715709), and NASA Planetary Atmospheres and Astronomy/Astrophysics Program Offices under contract

NAS7-100 to the Jet Propulsion Laboratory, California Institute of Technology, Pasadena, CA 91109, NAGW-649 to the University of Arizona, Tucson, AZ 85721, and NAGW-163 to the University of Southern California, Los Angeles, CA 90089.

## REFERENCES

- Ajello, J. M., & Franklin, B. 1985, *J. Chem. Phys.*, 82, 2519  
 Ajello, J. M., & Shemansky, D. E. 1985, *J. Geophys. Res.*, 90, 9845  
 Ajello, J. M., Shemansky, D., Kwok, T. L., & Yung, Y. L. 1984, *Phys. Rev.*, 29, 636  
 Ajello, J. M., Srivastava, S. K., & Yung, Y. L. 1982, *Phys. Rev. A*, 25, 2485  
 Ajello, J. M., et al. 1988, *Appl. Opt.*, 27, 890  
 Ajello, J. M., James, G. K., Franklin, B. O., & Shemansky, D. E. 1989, *Phys. Rev. A*, 40, 3524  
 Beswick, J. A., & Glass-Maujean, M. 1987, *Phys. Rev. A*, 35, 3339  
 Bethe, H. A., & Salpeter, E. E. 1977, in *Quantum Mechanics of One- and Two-Electron Atoms* (New York: Plenum/Rosetta), 284  
 Böse, N., & Linder, F. 1979, *J. Phys. B*, 12, 3805  
 Compton, R. N., & Bardsley, J. N. 1984, in *Electron-Molecule Collisions*, ed. I. Shimamura & K. Takayanagi (New York: Plenum), 275  
 Dieke, G. H. 1935, *Phys. Rev.*, 48, 610  
 Glass-Maujean, M., Guyon, P. M., & Breton, J. 1986, *Phys. Rev.*, 33, 346  
 Glass-Maujean, M., Frohlich, H., & Beswick, J. A. 1988, *Phys. Rev. Letters*, 61, 157  
 Glass-Maujean, M. 1989, *Phys. Rev. Letters*, 62, 144  
 Guberman, S. L. 1983, *J. Chem. Phys.*, 78, 1404  
 Guyon, P. M., Breton, J., & Glass-Maujean, M. 1979, *Chem. Phys. Letters*, 68, 314  
 Higo, M., & Ogawa, T. 1980, *Chem. Phys. Letters*, 75, 271  
 Karolis, C., & Harting, E. 1978, *J. Phys. B*, 11, 357  
 Khayrallah, G. A. 1976, *Phys. Rev. A*, 13, 1989  
 Landau, M., Hall, R. I., & Pichou, F. 1981, *J. Phys. B*, 12, 1003  
 Leventhal, M., Robiscoe, R. T., & Lea, K. R. 1967, *Phys. Rev.*, 158, 49  
 Malcolm, I. C., Dassen, H. W., & McConkey, J. W. 1979, *J. Phys. B*, 12, 1003  
 McLaughlin, R. W. 1977, Ph.D. thesis, University of Pittsburgh  
 Misakian, M., & Zorn, J. C. 1972, *Phys. Rev.*, 6, 1280  
 Mumma, M. J., & Zipf, E. 1971, *J. Chem. Phys.*, 55, 61  
 Pang, K. D., Ajello, J. M., Franklin, B., & Shemansky, D. E. 1987, *J. Chem. Phys.*, 86, 2750  
 Sharp, T. E. 1971, *Atomic Data*, 2, 119  
 Shemansky, D. E., Ajello, J. M., & Hall, D. T. 1985a, *ApJ*, 296, 765.  
 Shemansky, D. E., Ajello, J. M., Hall, D. T., & Franklin, B. 1985b, *ApJ*, 296, 774  
 Spezeski, J. J., Kalman, O. F., & McIntyre, L. C. 1980, *Phys. Rev.*, 22, 1906  
 Van Brunt, R. J., & Zare, R. N. 1968, *J. Chem. Phys.*, 48, 4304  
 van der Burgt, P. J. M., Westerveld, W. B., & Risley, J. S. 1989, *J. Phys. Chem. Ref. Data*, 18, 1757  
 Vroom, D. A., & de Heer, F. J. 1969, *J. Chem. Phys.*, 50, 580  
 Weingartshofer, A., Clarke, E. M., Holmes, J. K., & McGowan, J. W. 1975, *J. Phys. B*, 8, 1552  
 Weingartshofer, A., Ehrhardt, H., Hermann, V., & Linder, F. 1970, *Phys. Rev. A*, 2, 294  
 Zipf, E. C. 1984, in *Electron-Molecule Interactions and their Applications*, 1, ed. L. G. Christophorou (Orlando: Academic), 335